Pharm Res (2016) 33:1115–1125
DOI 10.1007/s11095-016-1856-x

RESEARCH PAPER

Simulation-Based Evaluation of PK/PD Indices for Meropenem Across Patient Groups and Experimental Designs

Anders N. Kristoffersson [1] • Pascale David-Pierson [2] • Neil J. Parrott [2] • Olaf Kuhlmann [2] • Thierry Lave [2] • Lena E. Friberg [1] • Elisabet I. Nielsen [1]

Received: 24 September 2015 / Accepted: 6 January 2016 / Published online: 19 January 2016

ABSTRACT

Purpose Antibiotic dose predictions based on PK/PD indices rely on that the index type and magnitude is insensitive to the pharmacokinetics (PK), the dosing regimen, and bacterial susceptibility. In this work we perform simulations to challenge these assumptions for meropenem and *Pseudomonas aeruginosa*.

Methods A published murine dose fractionation study was replicated *in silico*. The sensitivity of the PK/PD index towards experimental design, drug susceptibility, uncertainty in MIC and different PK profiles was evaluated.

Results The previous murine study data were well replicated with *f*T > MIC selected as the best predictor. However, for increased dosing frequencies *f*AUC/MIC was found to be more predictive and the magnitude of the index was sensitive to drug susceptibility. With human PK *f*T > MIC and *f*AUC/MIC had similar predictive capacities with preference for *f*T > MIC when short $t_{1/2}$ and *f*AUC/MIC when long $t_{1/2}$.

Conclusions A longitudinal PKPD model based on *in vitro* data successfully predicted a previous *in vivo* study of meropenem. The type and magnitude of the PK/PD index were sensitive to the experimental design, the MIC and the PK. Therefore, it may be preferable to perform simulations for dose selection based on an integrated PK-PKPD model rather than using a fixed PK/PD index target.

KEY WORDS antibiotic · dose selection · meropenem · pharmacometric · pseudomonas aeruginosa

ABBREVIATIONS

AUC	Area under the curve
c.i.	Continuous infusion
CL	Clearance
CL_{CR}	Creatinine CL
C_{max}	Maximum concentration
*f*AUC/MIC	Unbound AUC divided by the MIC
fC_{max}/MIC	Unbound C_{max} divided by the MIC
*f*T > MIC	Unbound time above the MIC
fu	Fraction unbound
h	Hour
i.v.	Intra venous
k	Rate constant
k_a	Absorption rate
MIC	Minimum inhibitory concentration
PD	Pharmacodynamic
PK	Pharmacokinetic
q	Dose interval
Q	Inter compartmental CL
R^2	Coefficient of determination
s.c.	Sub cutaneous
SCr	Serum creatinine
T	Time
$t_{1/2}$	Half-life (elimination)
$t_{1/2\beta}$	Half-life of the β-phase
TDM	Therapeutic drug monitoring
V	Volume
Vc	Central Volume (of distribution)
Vp	Peripheral volume (of distribution)
w	Week
WT	Weight

✉ Anders N. Kristoffersson
anders.kristoffersson@farmbio.uu.se

[1] Department of Pharmaceutical Biosciences, Uppsala Universitet, Box 591, Uppsala SE-751 24, Sweden

[2] F. Hoffmann-La Roche Ltd., Innovation Center Basel, Pharmaceuticals Sciences, Basel, Switzerland

INTRODUCTION

The effect of an antibiotic on the bacterial infection in a patient is dependent on the dosing regimen, and the pharmacokinetic (PK) and pharmacodynamic (PD) properties of the administered drug. The importance of understanding PKPD relationships is recognized by the regulatory authorities and PKPD studies are recommended to be included in antibacterial drug development programs in order to guide efficacious dosing regimens.(1–3) As the target of an antibiotic is an exogenous pathogen the PD activity of the drug may often be studied *in vitro*.(3) A commonly used measurement of the *in vitro* PD activity of antibiotics is the minimum inhibitory concentration (MIC). The MIC represents a point estimate of drug effect (typically measured after 18–24 h) and does not take into account the whole time course of bacterial growth and killing.(4) Another shortcoming is that the precision of the MIC value is limited, either by the dilution steps if derived in liquid culture media, or by the resolution of the antibiotic gradient if derived on solid media (e.g., Etest). A more complete description of drug activity is obtained from the effect on the bacteria over time in various *in vitro* systems in so called time-kill experiments.(5)

In order to guide the dosage of antibiotics, the MIC is often linked to a summary measure of the PK of the drug to create a PK/PD index.(6) The regularly used PK/PD indices are T > MIC – the fraction of the dosing interval that the drug concentration in plasma is higher than the MIC; AUC/MIC –the ratio of the area under the plasma concentration time curve to the MIC; C_{max}/MIC – the ratio of the maximum drug concentration in plasma to the MIC.(7) If the index was determined with regard to the unbound (free) concentration the prefix *f* is used. Commonly the relevant type and target magnitude of the PK/PD index for a drug-bacteria combination is decided using animal infection models in dose fractionation studies. In such studies the different PK/PD indices are derived for a wide range of exposures and dosing intervals and then correlated to the bacterial burden at 24 h.(4) A human dosing regimen is then suggested by extrapolating the results using *in silico* Monte Carlo simulations utilizing human PK models.(8)

The PK/PD indices share the limitations of the MIC value they are based on and carry the additional assumption that they are unaffected by differences in PK profiles, e.g., when extrapolating to different target populations. An alternative to PK/PD indices, which enable description of the whole time course of bacterial kill and growth, is to construct *in silico* PKPD models.(9) By linking such a model to a model of the human PK, dosing regimen selection may be performed to, for example, identify a regimen that achieves a fast bacterial kill (10,11) or suppression of resistance.(12) A semi-mechanistic model structure has previously been developed and shown to describe changes in bacterial counts over time as a function of concentration for several different antibiotics.(13) In the model the bacteria is assumed to exist in two states: either as growing drug-susceptible or resting drug-insusceptible bacteria. This allows the model structure to describe the biphasic killing often seen in time-kill studies (13) and to predict the inoculum effect (i.e., a reduction in bacterial killing at high inoculum) (9) which is observed for e.g. *Pseudomonas aeruginosa* exposed to carbapenems.(14) Additionally, the model structure has been used to characterize different mechanisms of resistance and has been employed for simulation of different dosing regimens.(12)

This model based approach has recently been applied to describe the kill and growth of two strains of *P. aeruginosa* of different susceptibility to meropenem.(15) Meropenem, like other β-lactams, is described as exhibiting a *f*T > MIC dependent effect.(6) A commonly cited magnitude for maximum bactericidal effect is 40% (16), however magnitudes exceeding this target are often required in clinical practice (17) and target requirements has been proposed to vary between individuals.(18) Therapeutic drug monitoring (TDM) has been suggested in order to ensure drug coverage up to 100% *f*T > MIC for β-lactams in critically ill patients with variable PK, however the benefit of such intervention has not been evaluated.(18) We believe a model based approach to dose selection may prove more robust compared to the fixed dosing target supplied by PK/PD indices. Thus in this work we predicted the *in vivo* observed PK/PD index of meropenem and *P. aeruginosa* utilizing *in silico* PKPD models based on *in vitro* time-kill curves to replicate a previously published *in vivo* dose fractionation study. After confirming the ability to predict the *in vivo* outcome the model was applied to investigate the expected impact on the type and magnitude of the PK/PD index of experimental design, uncertainty in the MIC, and differences in PK between patient populations.

METHODS

In this work, previously described meropenem PK models were combined with a PKPD model for the effect of meropenem on *P. aeruginosa* in order to simulate bacterial kill and growth in response to different dosage regimens. The predicted bacterial densities at 24 h were correlated with the values for the PK/PD indices derived according to standard methodology.(4)

PKPD Model

A longitudinal PKPD-model for meropenem and *P. aeruginosa* wild-type (ATCC27853, MIC 1 mg/L) and meropenem-resistant clinical isolate (ARU552, MIC 16 mg/L) was used in the simulations.(15) The model structure (Fig. 1) consists of two bacterial subpopulations, one susceptible (subpopulation

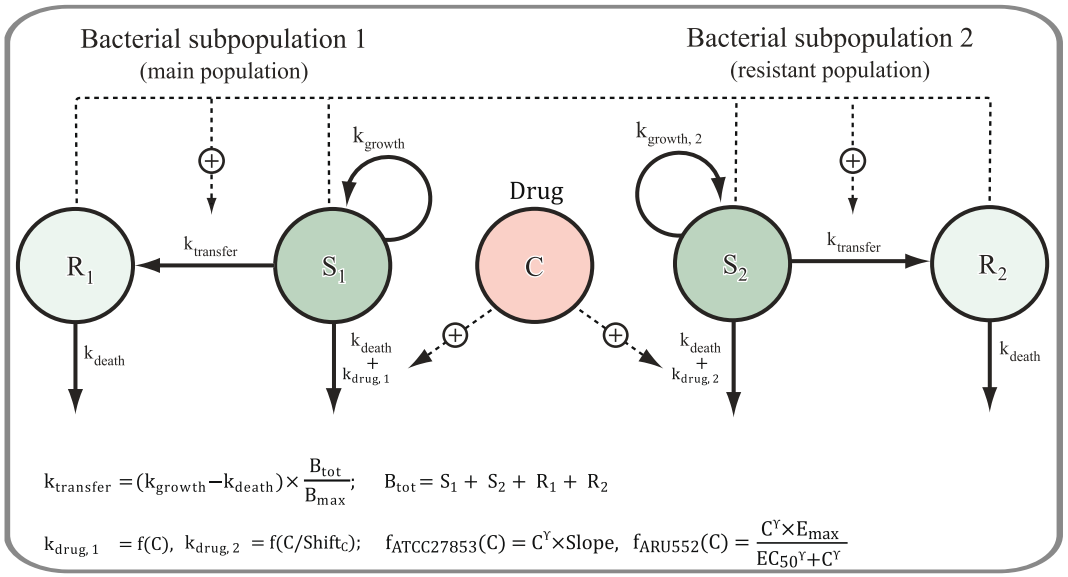

Fig. 1 Meropenem PKPD model developed for *Pseudomonas aeruginosa* (15). The model includes two bacterial subpopulations, one susceptible (subpopulation 1) and one pre-existing resistant (subpopulation 2) present at 0.15% of the start inoculum. The pre-existing resistant bacteria require 23.5 times higher ($Shift_C$) antibiotic concentration for effect. In each subpopulation the bacteria may exist in one of two discrete states: 1. Antibiotic susceptible (S) proliferating bacteria, 2. resting (R) non-proliferating bacteria being unsusceptible to the antibiotic. The bacteria enter the R state as a response to high population densities (R + S of both subpopulations). The drug effect is modelled as a power model for ATCC27853 and as a sigmoidal Emax model for ARU552. For definition of model parameters see Table I.

1) and one pre-existing resistant (subpopulation 2). The model parameters are reported in Table I. In each subpopulation the bacteria may exist in two states: proliferating antibiotic susceptible (S) bacteria and resting (R) non-proliferating bacteria unsusceptible to the antibiotic. The bacteria in the S state proliferate with rate k_{growth} and the bacteria enter the R state with rate $k_{transfer}$ as a response to high bacterial densities. Both states share the same natural death rate constant k_{death}. The drug action increase the death rate of the S state by rate k_{drug} and is modelled by a power model for ATCC27853 and a sigmoidal Emax model for ARU552. The two subpopulations share all parameters except k_{growth} (decreased for pre-existent resistant bacteria of strain ARU552) and the concentration required for effect (increased by $Shift_C$ for the pre-existent resistant bacteria). The residual error is included as an additive error on log scale with one component of the error being independent of other measurements (RES) and one component of the error shared with other replicates of measurements from the same culture vessel at the same time point (RRES). (19)

PK Models

A model described by Katsube *et al.* (20) was used to simulate PK profiles in mice. The model is based on data from a study where 5 week old female ICR mice infected with *P. aeruginosa* were given meropenem co-administered with cilastatin (which decreases meropenem CL in mice). The meropenem

Table I Parameters for the Meropenem PKPD Model for *Pseudomonas aeruginosa* Strains ATCC27853 and ARU552 (15)

Parameter	Description	ATCC27853	ARU552
B_{max} (CFU/mL)	Bacterial count in stationary phase	$1.29*10^9$	
k_{growth} (h^{-1})	Rate constant of bacterial growth	1.08	0.814
k_{death} (h^{-1})	Rate constant of bacterial natural death	0.179	
E_{max} (h^{-1})	Maximum kill rate constant	–	1.74
EC_{50} (mg/L)	Concentration that produces 50% of E_{max}	–	17.7
Slope (L/mg*h)	Slope drug effect	17.2	–
γ (−)	Hill factor in drug-effect relationship	0.376	2.79
Mut (%)	Fraction of pre-existing resistant bacteria	0.15	
$Shift_C$ (−)	Shift in concentration required for effect on pre-existing resistant bacteria	23.5	
$k_{growth,2}$ (h^{-1})	k_{growth} for pre-existing resistant bacteria	1.08	0.378
RES (%)	Residual error	164	
RRES (%)	Replicate residual error	8.74	

disposition was described by a one compartment model with first order absorption. Parameter values are reported in Table II.

For simulating the meropenem PK profile in an adult human population, a model by Li *et al.* (21) was used (Table II). This model is based on a large number of individual PK samples (1 to 12 samples per individual) from a total of 79 patients (age 18–93 years) treated for intra-abdominal infections or pneumonia. The meropenem disposition is described by a two compartment model with the covariates creatinine clearance (CL_{CR}) and age (Age) included on clearance (CL), and weight (WT) included on the central volume of distribution (Vc). CL_{CR} was calculated according to the Cockcroft-Gault equation.(24) Parameter values for a typical patient (CL_{CR} of 102 mL/min) and patients with augmented CL (CL_{CR} of 255 mL/min) and with renal dysfunction (CL_{CR} of 15 mL/min) are given in Table II.

The meropenem neonatal PK model by van den Anker *et al.* is based on data from 26 preterm (gestational age 29–36 w) and 15 term (gestational age 37–42 w) neonates hospitalized due to a known or presumed bacterial infection.(22) In this model the meropenem disposition is described by a two compartment model with covariates CL_{CR} and WT on CL. The parameter values used to simulate PK of a typical preterm neonate is reported in Table II.

Simulation Settings

The PK and PKPD models for meropenem were implemented and the unbound concentration-time profiles in the central compartment were used to drive the bacterial killing in the PKPD model. In mice the unbound fraction was set to 0.81 as determined in the murine PK study. In humans the protein binding was assumed to be negligible (21,22) and the unbound fraction was set to 1, see Table II. For each dosing regimen, the investigated PK/PD indices (*f*T > MIC, *f*AUC/MIC, *f*-Cmax/MIC) and the bacterial burden at 24 h were predicted (Fig. 2).

Simulated Mouse PK/PD Index Studies

For the simulated mouse dose fractionation studies the initial bacterial density was set to $10^{6.5}$ CFU/mL. The fraction of cells residing in the R state was computed to 3.6% by assuming that all bacteria started in the S state and then simulating bacterial growth during the inoculum procedure used by Sugihara *et al.* (23) Simulations of growth and kill of *P. aeruginosa* were performed using the PK for 5 week old male ICR mice (Table II). As the male ICR mice in the Sugihara study were expected to be heavier compared to the female ICR mice in the model by Katsube *et al.* allometric scaling (25) was applied to account for the expected (26) weight difference. All doses were simulated as s.c. bolus injections. In order to account for the MIC difference between the strain used in the *in vivo* study (*P. aeruginosa* 1246, MIC = 2 mg/L) and the strains in the modelled *in vitro* study (ATCC27853, MIC = 1 mg/L, and ARU552, MIC = 16 mg/L) the dose levels were adjusted to achieve the same steady state exposures, see Table III. The following scenarios were simulated (Table III): i) Original – replicating the dose fractionation

Table II Parameters for Meropenem PK Models Used for Simulating Concentration-Time Profiles for Mouse, and Human (adults and neonates). The Models were Parameterized in Terms of Absorption Rate Constant (ka; for mice studies only), Clearance (*CL*), Central Volume of Distribution (*Vc*), Inter Compartmental Clearance (*Q*), Peripheral Volume Of Distribution (*Vp*), and Fraction Unbound (*fu*). The Meropenem Elimination Half-Life ($t_{1/2}$) in Mice and the Half-Life of the Second Phase ($t_{1/2\ \beta}$) in Human are Given for Reference

Parameter	Mouse		Human			
	Female (20)	Male	Typical patient (21)	Augmented CL (21)	Renal dysfunction (21)	Preterm neonate (22)
ka (h^{-1})	10.2	10.2	–	–	–	–
CL (L/h)	0.033[a]	0.038[b]	14.6[c]	30[d]	5.0[e]	0.36[f]
Vc (L)	0.014 [a]	0.017[b]	10.8[c]	10.8[d]	10.8[e]	0.83
Q (L/h)	–	–	18.6	18.6	18.6	4.89[g]
Vp (L)	–	–	12.6	12.6	12.6	0.12[g]
fu (−)	0.81	0.81	1	1	1	1
$t_{1/2}$ (β) (h)	0.29	0.31	1.4	0.87	3.5	2.0

[a] calculated for a 24.4 g female mouse

[b] allometrically scaled to a 29.6 g male mouse (as used in Sugihara *et al.*(23)) using allometric exponents of 0.75 for CL and 1 for V

[c] calculated for a typical individual: WT = 70 kg (ideal body weight), Age = 35 years, Sex = Male, SCr = 1 mg/dl

[d] as [c] calculated for the lowest SCr observed = 0.4 mg/dl

[e] as [c] calculated for the highest SCr observed = 6.9 mg/dl

[f] calculated for CL_{CR} = 24.3 mL/min, WT = 1.87 kg

[g] values calculated from intercompartmental transfer rate constants and Vc

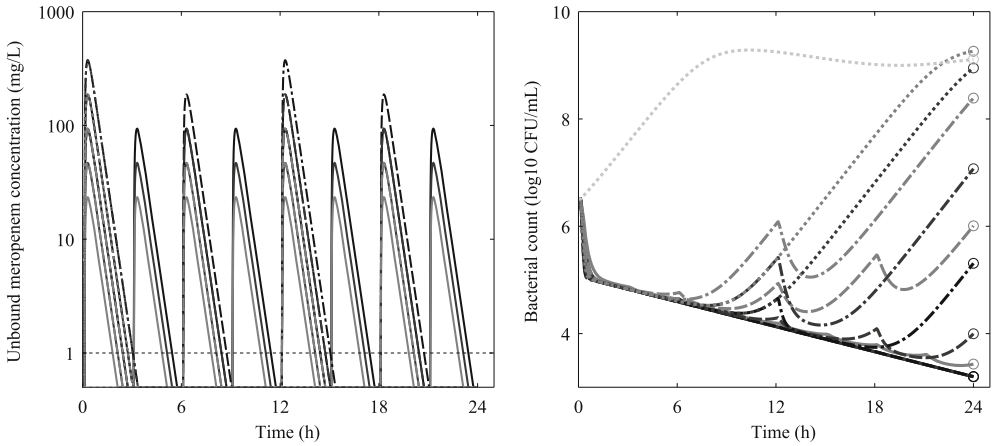

Fig. 2 Dose finding study for meropenem by Sugihara *et al*. (23) replicated in simulation for *Pseudomonas aeruginosa* ATCC27853 (MIC = 1 mg/mL). Left: simulated unbound meropenem concentration time profiles in mice predicted from PK by Katsube *et al*. (20), Right: The corresponding bacterial time-kill curves predicted by the PKPD model by Mohamed *et al*. (15) The simulated curves corresponds to doses of 0, 200, 400, and 800 mg/kg*day (indicated by colour from *light grey to black*) given once (*dotted*), twice (*dot-dash*), four-times (*dash*), and eight-times (*solid*) daily. All dose levels were administered in all dose intervals with the exception of the highest dose level (800 mg/kg*day) which in keeping with Sugihara *et al*. was not given once daily. The PK/PD indices (*f*T > MIC, *f*AUC/MIC, *f*Cmax/MIC) were computed with regard to the MIC (*Left*: *horizontal dashed line*) and correlated to the bacterial density at the study endpoint (*Right*: *circles*).

study by Sugihara *et al.* using the model for ATCC27853 , ii) 0.5 × MIC – as Original but with an assumed MIC of ATCC27853 set to 0.5 mg/L corresponding to a 0.5-fold lower MIC (underestimation, simulated susceptibility was not changed) , iii) 2 × MIC – as Original but with an assumed MIC of ATCC27853 set to 2 mg/L corresponding to a 2-fold higher MIC (overestimation, simulated susceptibility was not changed), iv) Resistant – as Original but simulating with the PKPD model parameters for the meropenem resistant strain ARU552 (MIC = 16 mg/L), v) Frequent – simulating with dose intervals of 4 h or lower plus continuous infusion to investigate the influence of dosing interval to the selected index, doses were adjusted to cover the full *f*T > MIC range (0–100%) for ATCC27853. Using shorter dose intervals compensate for the faster PK in mice compared to humans by bringing the ratio of elimination $t_{1/2}$ (and hence *f*T > MIC) to dosing interval closer to the corresponding situation in human. The simulations were performed using 10 times the sample size of the original *in vivo* study design, using the variability described by the residual error of the PKPD model in order to replicate the variability observed in the *in vivo* data. Variability in PK was assumed to be low in comparison to the PD variability and not included in the simulations.

Human PK/PD Index Simulations

The second part of the study consisted of simulations where the antibacterial effect was driven by the PK profile expected in humans, and are compiled in Table IV. The bacterial burden and the investigated PK/PD indices at 24 h were simulated in four human populations i) Typical patient, ii) Augmented CL, iii) Renal dysfunction, and iv) Preterm neonate. The same simulation settings as in the mouse simulations were applied, except that a wider range of concentrations and dosing intervals was used (Table IV) allowing for full characterization of the PK/PD index – effect relationship. In order to test the influence of the pronounced inoculum effect previously observed for meropenem (14), simulations were also performed with an increased initial bacterial density of 10^9 CFU/mL (scenario v, High inoculate). The initial fraction of cells in the resting state (R) was computed to 37% by following the same simulation procedure as previously, but allowing for a longer period of natural growth prior to start of treatment to reach the higher density. The doses were set to cover the range of unbound steady-state concentrations which achieve maximum bacterial suppression (eradication of all growing cells) to growth up to the carrying capacity of the system for all

Table III The Simulated Dose Fractionation Studies in Mice, All Doses were Administered as s.c. Bolus Except the Continuous Infusion (c.i.) of the Frequent Scenario

Scenario	Bacterial strain	Meropenem (mg/kg/day)	Dosing intervals (h)
i) Original	ATCC27853	800[a], 400, 200, 0	3, 6, 12, 24
ii) 0.5 × MIC	ATCC27853	400[a], 200, 100, 0	3, 6, 12, 24
iii) 2 × MIC	ATCC27853	1600[a], 800, 400, 0	3, 6, 12, 24
iv) Resistant	ARU552	12800[a], 6400, 3200, 0	3, 6, 12, 24
v) Frequent	ATCC27853	533, 267, 133, 50, 0	1, 2, 4, + c.i.

[a] In line with Sugihara *et al*. the highest daily dose was not included for the once daily dosing interval

Table IV The Simulated Dose Fractionation Studies in Humans. The Doses were Administered as 0.5 h i.v. Infusions Except the Continuous Infusion (c.i.)

Scenario	PK	Start bacterial burden (log10 CFU/mL)	Meropenem ($C_{ss,\ avg}$ x MIC)[a]	Dosing intervals (h)
Typical patient	Li *et al.* (21)	6.5	0.0156, 0.0313, 0.0625, 0.125, 0.25, 0.5, 1, 2 4, 8, 16, 32, 64	0, 4, 8, 12, 24, + c.i.
Renal dysfunction	Li *et al.* (21)	6.5		
Augmented CL	Li *et al.* (21)	6.5		
Preterm neonate	van den Anker *et al.* (22),	6.5		
High inocula	Li *et al.* (21)	9		

[a] Dosages achieving simulated average meropenem steady state concentrations as multiples of MIC

simulated scenarios. Meropenem was assumed to be administered as 0.5 h i.v. infusions. As no comparison was performed with *in vivo* data no variability was added to the simulated bacterial numbers and no inter individual variability was simulated in order to make the difference between indices clearer.

PKPD Index Determination

A sigmoid maximum effect (Emax) model was used to examine the relationship between each PK/PD index (*f*T > MIC, *f*AUC/MIC, *f*C_{max}/MIC) and the efficacy of the drug, measured as $\log_{10}$ bacterial density at 24 h. The Emax model was defined according to:

$$E = E_0 - \frac{PD_{max} \times X^{\gamma}}{X^{\gamma} + EX_{50}^{\gamma}}$$

where E is the PD endpoint ($\log_{10}$ bacterial burden at 24 h), E_0 is the zero effect value (maximum bacterial burden at 24 h), X is the value of the PK/PD-index, PD_{max} is the maximum effect (reduction in bacterial burden at 24 h), EX_{50} is the value of the PK/PD index required to achieve 50% of PD_{max}, and γ is the sigmoidicity factor.

The analysis was performed by the fit function in MATLAB, using the NonLinearLeastSquares method and the robust fit option. The coefficient of determination (R^2) was used to choose the PK/PD index with best correlation to bacterial density. The magnitude of the PK/PD indices required for bactericidal effect (here chosen as 99% killing from the bacterial burden at time 0, i.e., 2-log kill) was calculated from the fitted parameter values for each PK/PD index.

Software Details

MATLAB r2012a (The MathWorks, Inc., Natick, Massachusetts, United States) was used for simulation, nonlinear regression analysis, and plotting. WebPlotDigitizer 3.8 (http://arohatgi.info/WebPlotDigitizer) was used for digitizing data from published figures.

RESULTS

The relationships between the investigated PK/PD indices and the efficacy of the drug in mice (observed and predicted) are presented in Fig. 3. In the original *in vivo* study by Sugihara *et al.* (23) (Fig. 3, top panel) *f*T > MIC had the highest predictive value ($R^2 = 0.74$), while *f*AUC/MIC was the second best predictor ($R^2 = 0.38$). The magnitude of *f*T > MIC associated with a 2-log decrease from the initial bacterial density at 24 h was 45%. The result was well replicated *in silico*. For the Original scenario (strain ATCC27853, MIC = 1 mg/L) the predictive power was highest for *f*T > MIC ($R^2 = 0.77$) with a value of 37% required for 2-log decrease. *f*AUC/MIC was found to be a poor predictor ($R^2 = 0.33$).

The magnitude of *f*T > MIC was found to be sensitive to MIC misspecification. In the 0.5 × MIC scenario (strain ATCC27853, assumed MIC = 0.5 mg/L) the magnitude required for 2-log decrease increased to 52% ($R^2 = 0.73$). For the 2 × MIC scenario (strain ATCC27853, assumed MIC = 2 mg/L) the magnitude required for 2-log decrease was reduced to 23% ($R^2 = 0.77$). In addition to misspecification of the measured MIC the influence of larger MIC differences between strains of the same species was investigated. In the Resistant scenario (strain ARU552, MIC = 16 mg/L) a magnitude of 52% *f*T > MIC ($R^2 = 0.81$) was required for 2-log decrease. In all scenarios above *f*T > MIC was the best predictor of efficacy. However, by changing the experimental design by only studying dosing up to every 4th h in the scenario Frequent (strain ATCC27853, MIC = 1 mg/L) *f*AUC/MIC ($R^2 = 0.76$) became an equal or superior predictor of efficacy compared to *f*T > MIC ($R^2 = 0.73$). The values associated with 2-log decrease in this scenario were 45% *f*T > MIC and 60 *f*AUC/MIC.

The human PK/PD index simulations are presented in Fig. 4. As residual error variability was not included in the human simulations the correlations are typically greater compared to the mouse simulations and smaller differences in R^2 values can be considered to bear greater weight. For a typical patient *f*T > MIC and *f*AUC/MIC exhibit similar predictability

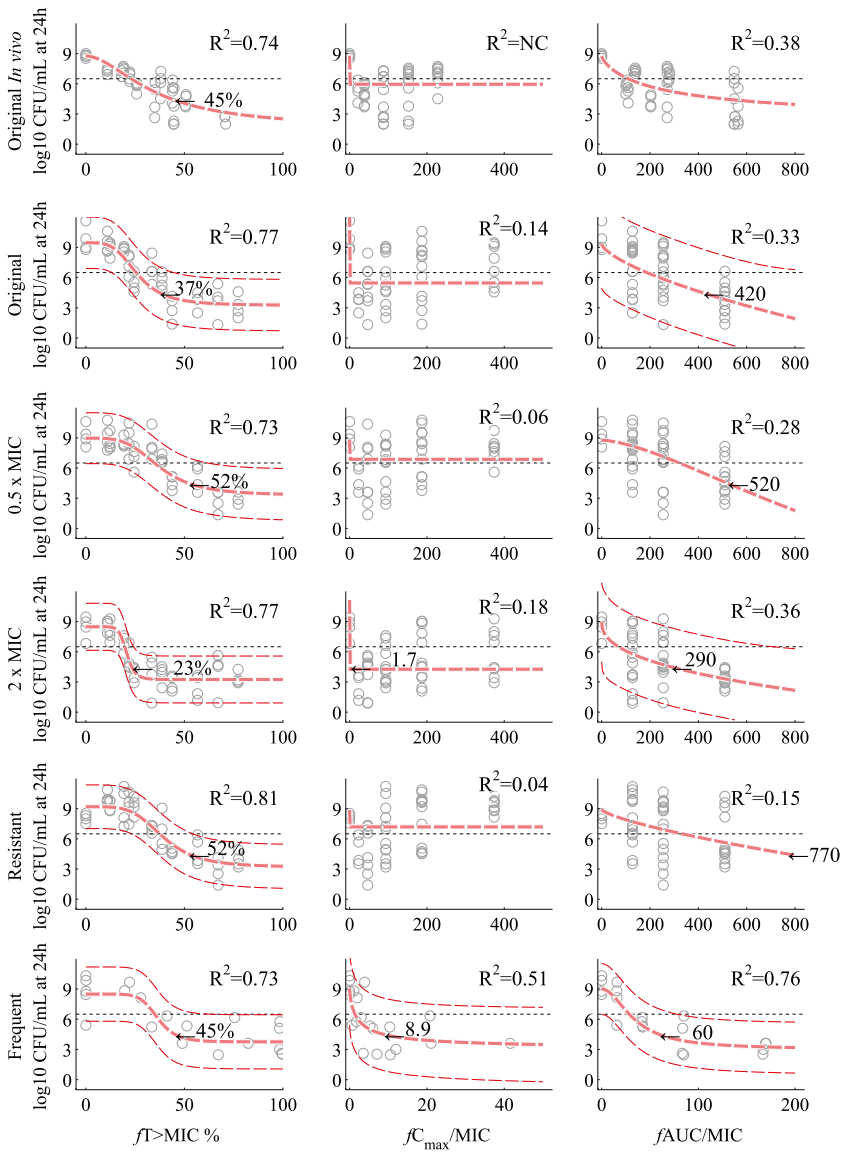

Fig. 3 Relationship between the PK/PD indices and the efficacy of meropenem against *P. aeruginosa* in mice. *Circles* – observations/predictions, *thin horizontal dashed line* - the viable cell count at start of therapy (as CFU/thigh or CFU/mL), *thick dashed line* – fitted Emax curve, *thin dashed lines* – 95% prediction interval around the fitted curve (shown for fits with R^2 values > 0.3). The magnitudes of the PK/PD index required for a 2-log decrease at 24 h from the viable cell count at start of therapy are indicated as well as the R^2 values of the curve fits. The curve fitting was performed simultaneously for all observations. In the plots only 10% of the simulated observations are shown in order to present the same number of observations as in the *in vivo* data. The top panel is reproduced with permission from *Antimicrobial Agents and Chemotherapy* (23).

for the bacterial density at 24 h ($R^2 = 0.98$ and $R^2 = 0.97$ respectively) while fC_{max}/MIC was less well correlated with efficacy ($R^2 = 0.88$). The magnitudes associated with 2-log decrease from initial bacterial density at 24 h were 43% $fT > MIC$, and 49 *f*AUC/MIC which is similar to the values for the Frequent dosing scenario in mice.

The result was only slightly affected when the terminal half-life was decreased from the typical value of 1.4 h to 0.87 h in the augmented CL population with *f*AUC/MIC becoming slightly less predictive ($R^2 = 0.94$). The simulated PK in renal dysfunction and preterm neonate populations exhibited a longer terminal half-life (3.5 h and 2.0 h respectively) compared to the typical value (1.4 h). In these cases *f*AUC/MIC had slightly higher correlation with efficacy ($R^2 = 1.00$ for renal dysfunction and $R^2 = 0.99$ for preterm neonatal), compared to $fT > MIC$ ($R^2 = 0.98$ for both populations). Compared to the typical adult patient the *f*AUC/MIC required for 2-log kill was the same or decreased (49 for renal dysfunction and 45 for preterm neonate) while the value of $fT > MIC$ was increased considerably (73% for renal dysfunction and 61% for preterm neonate).

Lastly, the effect of an increased bacterial density at the start of treatment was investigated for a typical patient by simulating a high initial inoculum of 10^9 CFU/mL. The maximum achievable suppression of bacterial number at 24 h (Emax) was reduced to 2.3 $\log_{10}$ CFU/mL for the high inocula compared to 5.9 $\log_{10}$ CFU/mL for the standard scenario. However, while the shape of the PK/PD index-effect relationship was changed the PK/PD index correlations were similar. The magnitudes associated with a 2-log decrease were in this setting 43% $fT > MIC$ and 68 *f*AUC/MIC.

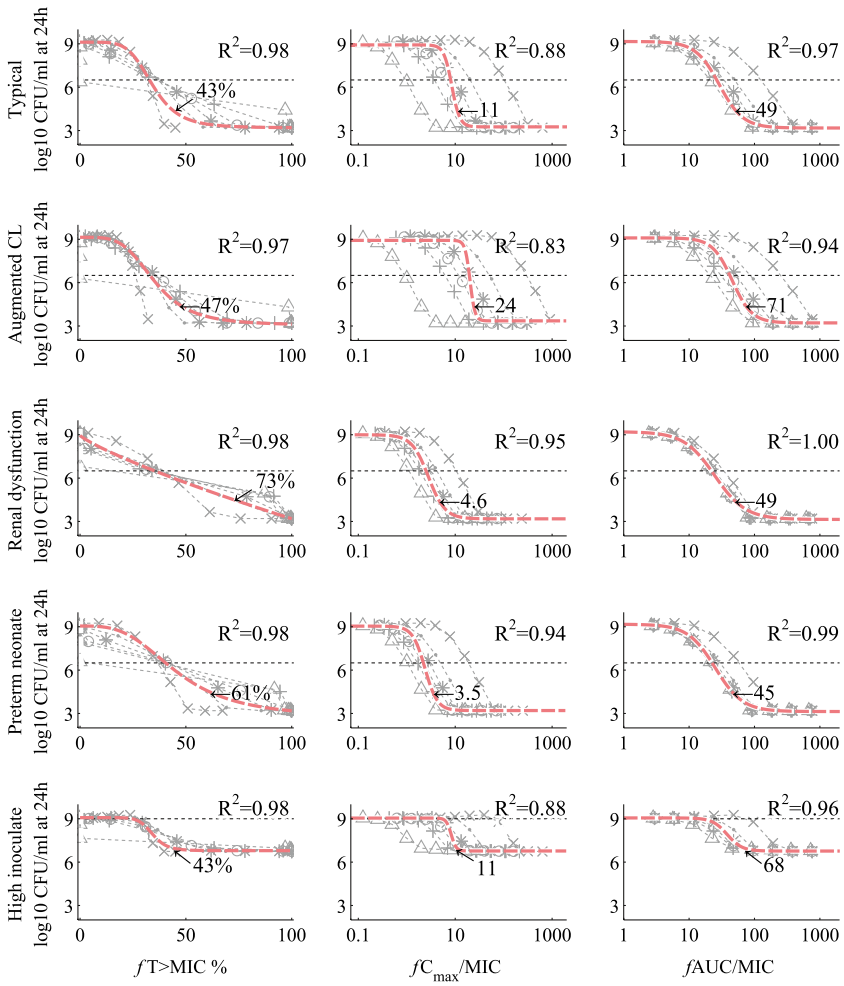

Fig. 4 Model predicted relationship between the PK/PD indices and the efficacy of meropenem against *Pseudomonas aeruginosa* in humans. Predictions for 0.5 h infusion q4h (*plus*), q6h (*circle*), q8h (*asterisk*), q12h (*point*), q24h (*cross*) and, continuous infusion (*pyramid*), *thin horizontal dashed line* - the viable cell count at start of therapy (as CFU/mL), *thick dashed line* – fitted Emax curve. Indicated in the figures is the magnitude of the PK/PD index required for a 2-log decrease at 24 h from the viable cell count at start of therapy and the R-square value of the curve fit. The curve fitting was performed simultaneously for all observations.

DISCUSSION

In this work a PKPD model based on *in vitro* time-kill data was combined with a literature PK model and found capable of predicting the *in vivo* outcome in a murine PK/PD index study of meropenem against *P. aeruginosa*. The simulated data was generally in good agreement with the *in vivo* observations. *f*-T > MIC was selected as the driver of efficacy with similar magnitudes required for 2-log kill as observed *in vivo* (37% *in silico* compared to 45% *in vivo*) (Fig. 3).

The PK/PD index most predictive of bacterial kill is known to be dependent on a complex interplay of PK and PD parameters such as the drug elimination rate and rates of kill and growth of the bacteria (27). In order to investigate how sensitive the selected index and target magnitude of meropenem is to variations in PK, PD and investigated dosages we expanded the *in silico* simulations in mouse and man.

The impact of the dilution step limited uncertainty in the MIC on the PK/PD index magnitude was exemplified by performing simulations where the MIC of strain ATCC27853 (observed as 1 mg/mL) was miss-specified either to 0.5 or 2 mg/L. The difference in magnitude of *f*T > MIC was found to be 29 percentage units (Fig. 3). This MIC derived uncertainty around the magnitude required for 2-log kill can be translated to an uncertainty in the human dose requirement. Assuming the distribution phase (alpha-phase) to be short and the dose large enough to exceed the MIC in at the start of the elimination-phase, the *f*T > MIC is proportional to the half-life of the elimination phase ($t_{1/2\beta}$) and the logarithm of the dose.(28) Hence a doubling of the dose will result in concentrations exceeding the MIC one $t_{1/2\beta}$ longer. Expressed differently, a shift in *f*T > MIC of duration ΔT h can be accomplished with a 2^(ΔT/ $t_{1/2\beta}$) fold dose adjustment. Considering an eight hourly (q8h) dosing regimen the difference in *f*T > MIC between the over- and underestimation scenarios corresponds to 2.3 h per dose interval. For a human $t_{1/2\beta}$ of 1.4 h the inherent uncertainty in the MIC measurement then translates to an approximately three-fold uncertainty in the dose needed to achieve a certain *f*T > MIC target.

Similar results were found when investigating strain differences. The resistant (29) (MIC = 16 mg/L) ARU552 strain required 15 percentage units longer *f*T > MIC compared to the susceptible (29) (MIC = 1 mg/L) ATCC27853 strain in order to achieve a 2-log decrease from the initial bacterial

count. Using the same assumption as above, the difference translates into an around 2-fold higher dose compared to what would be expected by performing dose adjustments according to the MIC of the resistant strain and the *f*T > MIC target determined for the susceptible strain. This finding challenges a core assumption of PK/PD indices, namely that the MIC may serve as an accurate marker for dose adjustments.(4) Additionally it puts into question how clinical breakpoints for antimicrobial therapy are derived as these investigations assume that the same target magnitude holds over a wide MIC distribution.(8)

As mentioned previously, *f*T > MIC is dependent on dose, dosing interval, and $t_{1/2}$,(28), thus differences in PK may affect the target and required magnitude. Sugihara *et al.* co-administered cilastatin and meropenem in order to bring the mouse meropenem half-life closer to human. However, even with the addition of cilastatin the observed mouse $t_{1/2}$ is almost five times faster than compared to the $t_{1/2\beta}$ of a typical adult human (Table II). The original study protocol by Sugihara *et al.* thereby includes dose intervals giving far lower *f*T > MIC compared to what would be seen in human (e.g., q4h dosing in mouse approximately corresponds to q20h in human with respect to %*f*T > MIC). The impact of the selected study design was tested in the Frequent scenario by decreasing the maximum dose interval in the simulated mouse study to 4 h, thereby bringing the ratio of elimination $t_{1/2}$ (and hence *f*T > MIC) to dosing interval closer to the corresponding situation in human. In addition, continuous infusion was included as it is an administration form thought to be beneficial for β-lactams.(30) The alternate experimental design shifted the most predictive PK/PD index from *f*T > MIC to *f*AUC/MIC, further highlighting the importance of PK and study design.

The influence of PK on the most predictive PK/PD index was also evident when simulating the expected outcome in different human populations (Fig. 4). Even though the predictive value of *f*T > MIC and *f*AUC/MIC was similar for all the simulated human scenarios, the most predictive PK/PD index shifted from the expected *f*T > MIC in the short $t_{1/2\beta}$ (0.9 h) augmented CL case to *f*AUC/MIC in the longer $t_{1/2\beta}$ (3.5 and 2.0 h respectively) cases of renal dysfunction and a preterm neonate. Similar results have previously been reported for benzylpenicillin for which a shift in the PK/PD index from *f*T > MIC in adults to *f*AUC/MIC in neonatals was observed in a simulation study.(31) These findings may seem surprising given the assumed time dependent effect of β-lactams. However, it has long been known that increasing the concentration of β-lactams up to 4 times the MIC leads to faster kill. (18,32) In addition, greater exposure above the threshold of selection for resistance will increase the ability to prevent regrowth by resistant subpopulations.(33) Combined these effects explain the interdependence of PK and dosing interval on the selected type and magnitude of the PK/PD index of meropenem where a longer $t_{1/2}$ compared to the investigated dosing interval for most doses achieves sufficient *f*T > MIC to supress regrowth of the main population and hence favours *f*AUC/MIC as the best predictor. Conversely, if the $t_{1/2}$ is short compared to the dosing interval *f*T > MIC is likely to be selected as the best predictor.

Of interest is not only which PK/PD index is most predictive, but also which magnitude is required for a certain effect. For the two longer $t_{1/2}$ populations (renal failure and neonate) a longer *f*T > MIC was required to meet the 2-log decrease target, while the *f*AUC/MIC target was the same or lower (Fig. 4). The discrepancy may be illustrated by changes in dose as above. For the renal dysfunction population the shift to higher *f*T > MIC (from 43 to 73%) matches the increase in $t_{1/2\beta}$ (from 1.4 to 3.5 h) indicating that no dose adjustment is expected to be necessary given a q8h dosing regimen. Conversely, as AUC is proportional to CL, the constant *f*AUC/MIC in face of a reduction in CL from 14.6 to 5 L/h indicate that the dose could be lowered three fold while retaining the same effect. Further, the magnitude required for a certain effect is not solely dependent on the PK, but rather – as for the most predictive index – on the interplay between PK and the choice of studied dosages. In the mouse simulations the magnitude of *f*AUC/MIC shifted from a high value in the Original scenario to a lower value when the humanised dosage was simulated in the Frequent scenario. This lower magnitude was also more close the *f*AUC/MIC magnitude predicted in the simulations with human PK.

While PK/PD indices are most commonly determined in newly infected animals where the bacteria are in the log-growth phase, the bacteria in a patient with an established infection might be close to stationary phase. The impact of an increased start bacterial density was investigated by PK/PD index simulation with an increased start density (10^9 CFU/mL, High inoculate scenario Table IV). A pronounced inoculum effect was predicted by the model structure, decreasing the maximum bacterial kill at 24 h by around 3 orders of magnitude (Fig. 4), which is similar to *in vitro* observations by Mizunaga *et al.*(14) The predicted inoculum effect suggests that *in vivo* PK/PD index studies may be overly optimistic regarding the ability to exceed a 2-log kill for meropenem in patients, and highlights the importance of incorporating a density dependent antibiotic drug effect in the PKPD model.

This study was based on a single PKPD model and antibiotic which could be seen as limiting the generalisability of the results. The ability to predict the commonly employed PK/PD indices for a range of antibiotics have however been confirmed previously (31), and the optimal PK/PD index has been shown to be mathematically dependent on the PK (27) which brings confidence to the presented results. For simplicity a 2-log kill target was used for making comparisons of drug effect between the studied scenarios, however the alternate 3-log kill target and the EX50 for each index (value for which

half the maximum effect is reached) were investigated with similar results except for the high inoculate scenario where 3-log kill was not predicted to be achievable.

It is interesting to note that while in all simulations with human PK $fT > MIC$ and $fAUC/MIC$ carried similar and high predictive value, the two most extreme dosages (iv-bolus once daily and continuous infusion) had the worst correlation with the fitted curves (Fig. 4), and were thus masking the correlation to the respective indices. If the drug effect was purely dependent on the time above some concentration or on the total drug exposure this would not be the expected outcome. The observation points to the important conclusion that the drug effect is not solely dependent on any single metric, but is affected by many factors such as time of administration in relation to start of infection and how rapidly the drug concentration changes in the site of infection.

A more versatile approach to dose regimen evaluation, capable of accounting for the dynamics of the drug and bacteria interplay, is to predict the longitudinal treatment effect in a patient. In this study PK and PKPD models were coupled to predict a single 24 h time-point in a single individual, but this approach can be expanded to cover the full time course of infection and treatment in a patient population. As no additional experimental data is needed (provided the PK and PKPD data covers the time interval and population variability of interest) the use of pre-clinical information in the design of efficient dosage regimens is maximized. Longitudinal model based dosage simulation allow the investigation of situations where rapid or sustained clearance of infection is desirable.(10–12) In comparison such investigations would require additional time points in *in vivo* systems, increasing cost and complexity and potentially resulting in different pharmacodynamic targets for each time point.

In this work PK differences between patient populations were investigated and the efficacy was assumed to be directly related to the drug plasma concentration. The assumption may hold for a well perfused muscle (such as the thigh infection model) but additional PK variability exists within a single patient due to differences in perfusion rates, permeability, and affinity of the drug in different body compartments. As previously proposed (18) and indicated by the presented results, such variability seems likely to affect the type and magnitude of the PK/PD-index. Physiologically based pharmacokinetic (PBPK) models (34) could be used in combination with PKPD models for dose optimization of infections at specific sites.

For various reasons, PKPD models based on *in vitro* data may not be able to fully substitute pre-clinical animal studies. However, if guided by *in silico* simulations animal studies may be used more sparingly in a confirmatory rather than exploratory way, bringing economical and ethical advantages. Additional advantages are found when evaluating drug combinations. Here the ability to explain the antibiotic interaction *in vitro* and to link the combined model with separately developed PK models enables rapid evaluation of combined dosing regimens,(15) which would be cumbersome using PK/PD indices.

CONCLUSION

A longitudinal *in vitro* based PKPD model was used to replicate a literature *in vivo* study and successfully predicted the type of PK/PD index and magnitude associated with efficacy for meropenem. The magnitude of the index, and hence the extrapolated human dose, was sensitive to experimental design, misspecification of the MIC, and the bacterial strain. In addition, based on the simulations, the PK/PD index in humans is expected to be PK dependent with associated implications for optimal dosing. Integration of PK and longitudinal PKPD models *in silico* may enable more robust and versatile dose finding than the traditionally used murine PK/PD index studies where a universal target is typically searched for. The integrated PK-PKPD models can readily be adapted to variable patient populations and infection sites to identify a target suitable for the situation of interest, with the ultimate goal of increasing the probability of safe and efficacious treatment for the individual patient.

ACKNOWLEDGMENTS AND DISCLOSURES

This work was in part supported by funding from F. Hoffmann-La Roche Ltd, Switzerland and by the Swedish Foundation for Strategic Research.

COMPLIANCE WITH ETHICAL STANDARDS

Transparency declarations The authors have no conflicts of interest related to the content of this study.

REFERENCES

1. European Medicines Agency. CHMP/EWP/2655/99 - Points to consider on pharmacokinetics and pharmacodynamics in the development of antibacterial medicinal products. http://www.ema.europa.eu/docs/en_GB/document_library/Scientific_guideline/2009/09/WC500003420.pdf. Accessed 29 Jan 2015.
2. European Medicines Agency. Concept Paper on revision of the points to consider on pharmacokinetics and pharmacodynamics in the development of antibacterial medicinal products (CHMP/EWP/2655/99) and conversion to a CHMP guideline. http://www.ema.europa.eu/docs/en_GB/document_library/Scientific_guideline/2014/02/WC500162135.pdf. Accessed 29 Jan 2015.
3. U.S. Food and Drug Administration. Developing antimicrobial drugs — General considerations for clinical trials (Draft Guidance). http://

www.fda.gov/Drugs/GuidanceComplianceRegulatoryInformation/Guidances/ucm064980.htm. Accessed 20 Jan 2015.
4. Craig WA. Pharmacokinetic/pharmacodynamic parameters: rationale for antibacterial dosing of mice and men. Clin Infect Dis: Off Publ Infect Dis Soc Am. 1998;26:1–10.
5. Gloede J, Scheerans C, Derendorf H, Kloft C. In vitro pharmacodynamic models to determine the effect of antibacterial drugs. J Antimicrob Chemother. 2010;65:186–201.
6. Lodise TP, Lomaestro BM, Drusano GL, P. Society of Infectious Diseases. Application of antimicrobial pharmacodynamic concepts into clinical practice: focus on beta-lactam antibiotics: insights from the Society of Infectious Diseases Pharmacists. Pharmacotherapy. 2006;26:1320–32.
7. Mouton JW, Dudley MN, Cars O, Derendorf H, Drusano GL. Standardization of pharmacokinetic/pharmacodynamic (PK/PD) terminology for anti-infective drugs: an update. J Antimicrob Chemother. 2005;55:601–7.
8. Mouton JW, Brown DF, Apfalter P, Canton R, Giske CG, Ivanova M, *et al.* The role of pharmacokinetics/pharmacodynamics in setting clinical MIC breakpoints: the EUCAST approach. Clin Microbiol Infect: Off Publ Eur Soc Clin Microbiol Infect Dis. 2012;18:E37–45.
9. Nielsen EI, Friberg LE. Pharmacokinetic-pharmacodynamic modeling of antibacterial drugs. Pharmacol Rev. 2013;65:1053–90.
10. Mohamed AF, Cars O, Friberg LE. A pharmacokinetic/pharmacodynamic model developed for the effect of colistin on Pseudomonas aeruginosa in vitro with evaluation of population pharmacokinetic variability on simulated bacterial killing. J Antimicrob Chemother. 2014;69:1350–1361.
11. Mohamed AF, Karaiskos I, Plachouras D, Karvanen M, Pontikis K, Jansson B, *et al.* Application of a loading dose of colistin methanesulfonate in critically ill patients: population pharmacokinetics, protein binding, and prediction of bacterial kill. Antimicrob Agents Chemother. 2012;56:4241–9.
12. Mohamed AF, Nielsen EI, Cars O, Friberg LE. A pharmacokinetic-pharmacodynamic model for gentamicin and its adaptive resistance with predictions of dosing schedules in newborn infants. Antimicrob Agents Chemother. 2012;56:179–88.
13. Nielsen EI, Viberg A, Lowdin E, Cars O, Karlsson MO, Sandstrom M. Semimechanistic pharmacokinetic/pharmacodynamic model for assessment of activity of antibacterial agents from time-kill curve experiments. Antimicrob Agents Chemother. 2007;51:128–36.
14. Mizunaga S, Kamiyama T, Fukuda Y, Takahata M, Mitsuyama J. Influence of inoculum size of Staphylococcus aureus and Pseudomonas aeruginosa on in vitro activities and in vivo efficacy of fluoroquinolones and carbapenems. J Antimicrob Chemother. 2005;56:91–6.
15. Mohamed AF, Kristoffersson AN, Karvanen M, Cars O, Nielsen EI, Friberg LE. Interaction of colistin and meropenem on a wild-type and a resistant strain of pseudomonas aeruginosa in-vitro as quantified in a mechanism-based model. J Antimicrob Chemother (in press).
16. Drusano GL. Prevention of resistance: a goal for dose selection for antimicrobial agents. Clin Infect Dis: Off Publ Infect Dis Soc Am. 2003;36:S42–50.
17. Roberts JA, Paul SK, Akova M, Bassetti M, De Waele JJ, Dimopoulos G, *et al.* DALI: defining antibiotic levels in intensive care unit patients: are current beta-lactam antibiotic doses sufficient for critically ill patients? Clin Infect Dis: Off Publ Infect Dis Soc Am. 2014;58:1072–83.
18. Huttner A, Harbarth S, Hope WW, Lipman J, Roberts JA. Therapeutic drug monitoring of the β-lactam antibiotics: what is the evidence and which patients should we be using it for? J J Antimicrob Chemother. 2015;70:3178–3183
19. Karlsson MO, Beal SL, Sheiner LB. Three new residual error models for population PK/PD analyses. J Pharmacokinet Biopharm. 1995;23:651–72.
20. Katsube T, Yamano Y, Yano Y. Pharmacokinetic-pharmacodynamic modeling and simulation for in vivo bactericidal effect in murine infection model. J Pharm Sci. 2008;97:1606–14.
21. Li C, Kuti JL, Nightingale CH, Nicolau DP. Population pharmacokinetic analysis and dosing regimen optimization of meropenem in adult patients. J Clin Pharmacol. 2006;46:1171–8.
22. van den Anker JN, Pokorna P, Kinzig-Schippers M, Martinkova J, de Groot R, Drusano GL, *et al.* Meropenem pharmacokinetics in the newborn. Antimicrob Agents Chemother. 2009;53:3871–9.
23. Sugihara K, Sugihara C, Matsushita Y, Yamamura N, Uemori M, Tokumitsu A, *et al.* In vivo pharmacodynamic activity of tomopenem (formerly CS-023) against Pseudomonas aeruginosa and methicillin-resistant Staphylococcus aureus in a murine thigh infection model. Antimicrob Agents Chemother. 2010;54:5298–302.
24. Cockcroft DW, Gault MH. Prediction of creatinine clearance from serum creatinine. Nephron. 1976;16:31–41.
25. West GB, Brown JH, Enquist BJ. A general model for the origin of allometric scaling laws in biology. Science. 1997;276:122–6.
26. Jonsson EN, Wade JR, Karlsson MO. Comparison of some practical sampling strategies for population pharmacokinetic studies. J Pharmacokinet Biopharm. 1996;24:245–63.
27. Kitamura Y, Yoshida K, Kusama M, Sugiyama Y. A proposal of a pharmacokinetic/pharmacodynamic (PK/PD) index map for selecting an optimal PK/PD index from conventional indices (AUC/MIC, Cmax/MIC, and TAM) for antibiotics. Drug Metab Pharmacokinet. 2014;29:455–462.
28. Turnidge JD. The pharmacodynamics of beta-lactams. Clin Infect Dis: Off Publ Infect Dis Soc Am. 1998;27:10–22.
29. EUCAST. Meropenem - Rationale for the EUCAST clinical breakpoints. www.eucast.org. Accessed 29 Jan 2015.
30. MacGowan A. Revisiting Beta-lactams - PK/PD improves dosing of old antibiotics. Curr Opin Pharmacol. 2011;11:470–6.
31. Nielsen EI, Cars O, Friberg LE. Pharmacokinetic/pharmacodynamic (PK/PD) indices of antibiotics predicted by a semimechanistic PKPD model: a step toward model-based dose optimization. Antimicrob Agents Chemother. 2011;55:4619–30.
32. Craig W, Ebert S. Killing and regrowth of bacteria in vitro: a review. Scand J Infect Dis Suppl. 1989;74:63–70.
33. Drusano G, Lodise T, Melnick D, Liu W, Oliver A, Mena A, *et al.* Meropenem penetration into epithelial lining fluid in mice and humans and delineation of exposure targets. Antimicrob Agents Chemother. 2011;55:3406–12.
34. Rowland M, Peck C, Tucker G. Physiologically-based pharmacokinetics in drug development and regulatory science. Annu Rev Pharmacol Toxicol. 2011;51:45–73.